Published in final edited form as:
Cryst Growth Des. 2010 November ; 10(11): 4815–4822. doi:10.1021/cg100696r.

Tooth enamel proteins enamelin and amelogenin cooperate to regulate the growth morphology of octacalcium phosphate crystals

Mayumi Iijima[a], **Daming Fan**[b], **Keith M. Bromley**[b], **Zhi Sun**[b], and **Janet Moradian-Oldak**[b,*]
[a]Dental Materials Science, Asahi University School of Dentistry, Gifu, Japan

[b]Center for Craniofacial Molecular Biology, University of Southern California, LA, CA, USA.

Abstract

To examine the hypothetical cooperative role of enamelin and amelogenin in controlling the growth morphology of enamel crystals in the post-secretory stage, we applied a cation selective membrane system for the growth of octacalcium phosphate (OCP) in the truncated recombinant porcine amelogenin (rP148) with and without the 32kDa enamelin fragment. Enamelin alone inhibited the growth in the *c*-axis direction more than rP148, yielding OCP crystals with the smallest aspect ratio of all conditions tested. When enamelin was added to the amelogenin "gel-like matrix", the inhibitory action of the protein mixture on the growth of OCP in the *c*-axis direction was diminished, while that in the *b*-axis direction was increased. As a result, the length to width ratio (aspect ratio) of OCP crystal was markedly increased. Addition of enamelin to amelogenin enhanced the potential of amelogenin to stabilize the amorphous calcium phosphate (ACP) transient phase. The ratio of enamelin and amelogenin was crucial for stabilization of ACP and the growth of OCP crystals with larger aspect ratio. The cooperative regulatory action of enamelin and amelogenin was attained, presumably, through co-assembling of enamelin and amelogenin. These results have important implications in understanding the growth mechanism of enamel crystals with large aspect ratio.

Keywords

octacalcium phosphate; enamelin; amelogenin; hydroxyapatite; enamel; amorphous calcium phosphate

Introduction

Tooth enamel formation is a classic example of cell- and matrix-mediated biomineralization in which the spatial regulation of crystal nucleation, growth and organization is highly controlled by the extracellular matrix proteins and glycoprotein constituents [1-3]. The

[*]**Corresponding author**: Janet Moradian-Oldak, 2250 Alcazar St., Los Angeles, CA, 90033, joldak@usc.edu, Tel: 323-442-1759, Fax:323-4422981.
Mayumi Ijima: iijima@dent.asahi-u.ac.jp
Daming Fan: Daming@usc.edu
Keith M. Bromley: kbromley@usc.edu
Sun Zhi: zhisun@usc.edu
Janet Moradian-Oldak: Joldak@usc.edu

Supporting Information Available Figure S1: Qualitative analysis of the amount of ACP in different samples: Overlap of X-ray diffraction pattern of OCP crystals grown in 10% rP148 with XRD profiles of 4μg/ml enamelin in 10% rP148 (rP148+4En), 10μg/ml enamelin in 10% rP148 (rP148+10En), 40μg/ml enamelin in 10% rP148 (rP148+40En) and (E) 40μg/ml enamelin (40En).

resulting biocomposite tissue has a uniquely organized hierarchical structure composed of extremely long carbonated apatite crystals. The unusually elongated crystals are arranged parallel to each other in their *c*-axial direction making the prisms or rod structures[4-7]. The characteristic enamel crystals are different in morphology from those of bone and dentin that are small and plate-like shaped. Amelogenin protein is the major component of the continuously secreted enamel extracellular matrix that controls the mineralization of enamel crystals[8]. *In vitro*, amelogenin molecules self-assemble to form nanospheres and higher order structures whose size distribution is dependent on pH and protein concentration[9-12]. *In vivo*, amelogenin assemblies have been identified along the growing mineral crystallites at the very early stages of tooth enamel formation and have been proposed to constitute the basic building unit of the enamel matrix[13,14]. In addition, *in vitro* evidence concerning the functional role of amelogenin in mineral formation has been accumulated. Specifically, amelogenin has been shown to accelerate the nucleation kinetics and induce ordering of apatite nanocrystallites[11,15-18], the charged hydrophilic C-terminal domain has been shown to be essential for the alignment of crystals into parallel arrays[18], and native phosphorylated amelogenin has been shown to stabilize amorphous calcium phosphate (ACP), while inhibiting precipitation of other calcium phosphates[19]. The above experimental evidence strongly supports the notion that amelogenin exerts control over the morphology, organization, and directionality of apatite crystals.

Enamelin, the largest known enamel protein, is a minor component of the matrix (1 to 5%) and is absolutely essential for formation of normal enamel tissue[20-22]. Porcine enamelin is secreted as a 186-kDa (1104 aa) glycoprotein. This acidic glycoprotein, like amelogenin, is processed immediately following secretion producing intermediate products (155 kDa, 145 kDa, 89 kDa) that are not stable and found only near the enamel surface [23-26]. One stable proteolytic intermediate fragment that accumulates to about 1% is the 32kDa enamelin, which has a strong affinity to adsorb onto the enamel crystals and is highly conserved across species27. Mutations in *ENAM* gene results in defective enamel, specifically hypoplastic form of autosomal dominant *amelogenesis imperfecta (AI)*, and a diverse group of genetically altered conditions. While the presence of enamelin was shown to be critical for the mineralization of normal enamel[23], details on the molecular mechanisms of its functions in controlling enamel crystal formation are still lacking. Interestingly, some *AI*-causing mutations in *ENAM* gene have been described to be within the 32 kDa enamelin segment [28-29]. *In vitro* studies have shown that the 32kDa enamelin fragment can promote the nucleation of apatite crystals when added to an amelogeningelatin mixture and can also induce elongation of apatite crystals grown in agarose gel[23-30]. Moreover, enamelin has been shown to directly interact with amelogenin, change its conformation, stabilize oligomers and partially dissociate amelogenin nanospheres[31]. Such observations have led us to the hypothesis that amelogenin and enamelin cooperate to function together in controlling the nucleation and growth of enamel crystals.

Recent studies have confirmed that in many mineralizing systems, an amorphous phase is the precursor to the crystalline mineral[32-36]. Interestingly, at the very early stage of forming tooth enamel, ribbon-shaped amorphous calcium phosphate (ACP) materials were identified in between the amelogenin-rich protein matrix[36]. With the progress of mineralization (in deeper enamel) the ACP converted to thin crystalline of apatite. These observations further supported the view that amelogenin is not only critical for controlling mineral morphology, but also mineral phase and organization. It has been proposed that cooperative interaction between assembling amelogenin and forming mineral is the underlying mechanism for the formation of organized enamel-like apatite crystals[11,15,17,18,37]. Remarkably, based on *in vitro* crystal growth experiments that were performed using the constant composition method, it was found that elongated ribbon-like crystals similar to enamel crystals could be

formed through the transient amorphous phase, under low super-saturation, and even low concentrations of amelogenin[17].

Previous studies on the spontaneous precipitation of ACP and its subsequent transition into apatite, revealed that the kinetically favored OCP was the first crystalline phase, which formed in a very close contact with the ACP particle surface[38-43]. The ability of OCP to incorporate water molecules and ions other than Ca^{2+} and PO_4^{3-} as structural components enables OCP to function as an apatite crystal precursor[44-45]. As the lifetime of OCP was usually very short, OCP was recognized as a labile intermediate. This transformation from OCP to apatite appears to be *in situ* and occurs via a solid-state rearrangement[44-46]. As OCP has been identified as a transient phase for enamel crystals, we have been studying the mechanism of the elongated growth of OCP crystals using a dual membrane experimental device where ionic diffusion was controlled by a cation-selective membrane and a dialysis membrane[47-52]. We have previously shown that 1) oriented OCP crystals preferentially grew in the c-axis direction on the membrane[47]; 2) amelogenin increased the aspect ratio of OCP crystal through the preferential interaction with the side faces of OCP[48-51] (this was true of both native and recombinant full-length amelogenins, and also true of both types of truncated amelogenin); 3) when fluoride was added to amelogenin, oriented prism-like apatite crystals with a large aspect ratio were formed[51-52]. Most importantly, we have shown that recombinant mouse amelogenins (rM179 and rM166) interacted with OCP crystal faces similarly in the concentration range of 1-10%. Later, we confirmed that recombinant porcine amelogenins (both rP172 and rP148) had the same effect on the morphology of OCP as rM179 and rM166. The degree of interaction of all of the tested types of amelogenin with OCP crystal faces was in the order (010) > (001) > (100). Thus, the aspect ratio of OCP was increased by amelogenins regardless of the type of amelogenin being native or recombinant. The presence of the hydrophilic carboxy-terminal or the phosphate group did not seem to affect the preference of amelogenin interaction with OCP crystal faces.

Here, using the same dual membrane system we applied a mixture of 10%(w/v) recombinant porcine amelogenin (rP148) and the native 32kDa enamelin fragment to examine the hypothesis that amelogenin and enamelin cooperate to control the elongated crystal growth of OCP. rP148 is an analogue to the 20kDa fragment of porcine amelogenin (P148), which is the prominent component of the enamel matrix during crystal development. It is a partially degraded product of full-length amelogenin, lacking the hydrophilic C-terminal and is therefore relatively hydrophobic. The use of recombinant protein in this study is necessary and justified because of two primary reasons. Firstly, recombinant porcine amelogenin rP148 can be expressed in our laboratory with a higher than 98% purity. This means it is free of contaminants such as enamel proteinases and non-amelogenin proteins such as enamelin. This is important because high level of purity and homogeneity are rarely obtained with large quantities of native amelogenins isolated from developing extracellular enamel matrix[53]. Secondly, the differences between native amelogenin P148 and recombinant rP148 is minimal in that the latter only lacks one phosphate on serine 16 and the N-terminal methionine 54. Moreover, as noted above, we have published numerous papers in which we reported the similarity of the effects of both native and recombinant amelogenin on the growth of OCP crystals [48-49]. It is noteworthy that due to the complex nature of enamelin (highly glycosylated and phosphorylated) and despite significant efforts by many investigators, a stable expression system for recombinant enamelin is not yet available[55]. We therefore used an enamelin fragment isolated from developing porcine enamel. The 32kDa enamelin fragment is the most stable fragment among a series of cleavage products. It is hydrophilic and acidic, and has two phosphorylated serines and three glycosylated asparagines[23,27,56]. Immunochemistry studies have shown a prominent presence of 32kDa enamelin in the inner layer of crystallite-containing rod and inter-rod

areas of enamel matrix57, indicating the co-localization of the 32kDa enamelin and the 20kDa amelogenin. More than 95% of the extracellular matrix is made up of amelogenin, which has an estimated concentration of 30% w/v (300mg/ml). While the amount of enamelin in the extracellular matrix has been estimated to be about 1-5%, the local concentration of the 32kDa fragment is not known precisely58,59. Because of limitations in amelogenin solubility we used only a 10% (w/w) amelogenin in our *in vitro* system [60]. By applying various biophysical techniques, we have previously demonstrated that recombinant amelogenin and native 32kDa enamelin interact directly *in vitro*[31]. Consequently, this system was established to be appropriate for our structural and functional studies.

Experimental Section

Preparation of amelogenin (rP148) and enamelin (En)

The recombinant porcine Amelogenin rP148 was expressed in *Escherichia coli*, purified using RP-HPLC, and characterized as previously described54,[61]. rP148 is analogous to the major amelogenin proteolytic product (P148 or the “20k”), lacking phosphate group on Ser 16 and a Met at the N-terminal, but containing a Met at the C-terminal. The 32kDa enamelin was extracted from unerupted 2nd and 3rd mandibular molars of six-month-old pig jaws, purified and characterized as described previously following the method described by Yamakoshi, et al. [27, 31, 62]. Samples were scraped from 2nd and 3rd unerupted molars of freshly dissected six-month-old pig jaws (Farmers John Clougherty Co., Los Angeles, CA, USA) through Sierra For Medical Sciences (Santa Fe Springs, CA, USA). The pooled enamel samples were homogenized in 50 mM Sørensen buffer (pH 7.4) with proteinase and phosphatase inhibitors. This extraction process was repeated three times. The combined supernatant was processed and purified by reverse-phase high performance liquid chromatography (RP-HPLC) as reported previously[62]. The purified 32kDa enamelin was characterized by sodium dodecyl sulfate-polyacrylamide gel electrophoresis (SDS-PAGE), stains-all staining and Edman degradation62.

Crystal growth

All chemicals used were reagent grade and all solutions were prepared with deionized and double distilled water (dd-water). Crystal growth of OCP was carried out in a gel-like matrix of rP148 and enamelin using a dual membrane system used in our previous studies47-52,63. Briefly, the reaction chamber was composed of a cation-selective membrane (CMV, Asahi Glass Co.) and a dialysis membrane (Visking Cellulose Tubing; pore size of 2.4nm; Union Carbide Co.). The crystallization solutions used were 10mM $Ca(CH_3COO)_2{\cdot}H_2O$ and 10mM $NH_4H_2PO_4$ + $(NH_4)_2HPO_4$ (1:1 molar ratio). The Ca and PO_4 solutions were adjusted with dilute HCl solution to pH6.5 at 37 °C before being used. After three days of reaction, the pH of Ca solution decreased from 6.5 to 5.88-5.95 and that of PO_4 solution decreased to 6.47-6.49. The larger pH decrease of the Ca solution is ascribed to the permionic selectivity of the cation selective membrane. From the calcium acetate solution, Ca^{2+} ions diffuse into the phosphate solution through the membrane, while CH_3COO^- ions cannot pass through the membrane. Thus, with the progress of the reaction, the amount of the acetic acid increased in the Ca solution and the pH of the Ca solution decreased. On the other hand, in the PO_4 solution, with the progress of the OCP deposition on the membrane, NH_4^+ and H^+ ions were produced in the PO_4 solution. However, due to their buffering effect, the change in pH was small. Enamelin stock solution was made by mixing 2.8μg of 32kDa enamelin and 70μl of dd-water (40μg/ml: 40En). The solution was preserved in a freezer and thawed before being used. A solution of 10%w/v rP148 was made by adding 14μl of ice-cold dd-water to a pre-weighed amount of rP148 (about 1.4mg). A solution of 10%w/v rP148 and 32kDa enamelin (represented as rP148+40En) was made by adding 14μl of cold 40En solution to a pre-weighed amount of rP148 (about 1.4mg). This process was

repeated with different concentrations of enamelin, creating 10% w/v rP148 solutions containing 10 μg/ml (10En) and 4 μg/ml (4En) enamelin. The 10% rP148 solution without enamelin and the enamelin solution alone (40μg/ml: 40En) without amelogenin were also used to grow crystals. Crystal growth experiments were carried out at 37 °C for 3 days under gentle stirring. After the reaction, the gel that was still fixed on the membrane was rinsed superficially with dd-water, frozen at -20 °C, and subsequently lyophilized.

Characterization of mineral phase

Crystals grown on the membrane were identified by an X-ray diffractometer (XRD) (RINT2500, 56kV, 200mA, CuK_{α}, Rigaku). Since the crystals grew tightly on the membrane in many cases, it was difficult to remove the products from the membrane. Therefore, the crystals were fixed on a sample holder with the membrane still attached. We used a non-reflective quartz holder that was cut from a quartz single crystal in a specific direction, so as not to cause XRD reflections at least up to 60 degree in two theta. The morphology of the crystals was observed by a scanning electron microscope (SEM) (S4500, 5kV, Hitachi). Crystal length (L), width (W) and thickness (T) were measured on SEM micrographs. To avoid parallax error, only crystals whose faces were parallel to the imaging direction were measured. Around 100 measurements were performed for each dimension and their means, standard deviations, and L/W and W/T ratios were calculated. The values were compared by applying the t-test (Welch's method) at α=0.05 using Microsoft Excel 2003.

For a qualitative estimation of the percentage of amorphous phase yielded by the addition of enamelin to 10% rP148, the X-ray diffraction pattern of the product grown in 10% rP148 was overlayed onXRD profiles of the crystals grown in 4μg/ml enamelin in 10% rP148 (rP148+4En), 10μg/ml enamelin in 10% rP148 (rP148+10En), 40μg/ml enamelin in 10% rP148 (rP148+40En) and 40μg/ml enamelin (40En) (Fig. 1 Supplementary Material).

EDXA (Energy Dispersive X-ray Analysis) mapping was performed on a JEOL JSM-7001F scanning electron microscope equipped with an EDAX Apollo X Silicon Drift Detector. The data was analyzed using EDAX Genesis software. Samples were placed onto adhesive carbon pads on aluminium stubs and were subsequently coated in gold using a Cressington 108 sputter coater.

Results and Discussion

We used a membrane system in which the one-directional Ca^{2+} ion diffusion allows the OCP crystals to grow preferentially in their *c*-axis direction [47,64]. As a result, the aspect ratio of the crystals grown on the membrane was larger than those grown in a solution system without the membrane. Amelogenin rP148 and the 32kDa enamelin had a synergic effect on changing the morphology of OCP crystals. Figure 1 summarizes the XRD patterns of the products formed in 10% rP148 only, enamelin only, and the mixture of rP148 and enamelin (rP148+4En, rP148+10En, rP148+40En). The primary products in all samples were identified as OCP. Notably, the 100 reflection at 2θ=4.7°, the 010 and 002 reflections, respectively, at 2θ=9.8° and 2θ=26° of OCP were apparent in all products. The broad diffraction in the range from 12° to 20° was due to the membrane. The broad diffraction in the range from 20° to 40° could be due to some amorphous material, because ACP obtained from pure calcium phosphate solution without any additives gives similar diffraction pattern with a broad maximum at about 30°[31]. Since many reflections of OCP overlap with those of apatite at 2θ >10° we cannot rule out the presence of HAP together with OCP in the final product. The characteristic 100, 200 and 010 reflections of OCP were important for identification of the mineral phase in the product, while the relative intensity of the peaks provided information on crystal orientation. It was noted that the intensity ratio of 100 and

002 decreased as enamelin content increased. It was reported that with the progress of the growth of OCP in length, the XRD intensity of the 002 and the 004 reflections increased. This finding confirmed that OCP grew in the *c*-axis direction resulting in the formation of crystals with ribbon-like morphology. This observation suggested that the degree of crystal arrangement/orientation was improved with increasing enamelin concentration in the gel-like matrix. The presence of additional diffraction peaks in the rP148+10En and rP148+40En confirms higher crystallinity and improved orientation of the OCP crystals[65].

As shown in the SEM image in figure 2 the crystals grown in the mixture of rP148+10En and rP148+40En were narrower than those grown in 10% rP148 only (Fig.2a), or 40En only (Fig.2b). Based on the 002 and 004 reflections, the XRD confirmed that the crystals extended in the *c*-axis direction of OCP. The mechanism of the growth process of OCP on the membrane has been investigated previously, using XRD and SEM[64].

The mean values and standard deviations (SD) of length, width, and thickness of crystals, as well as calculated length to width ratio (L/W) and width to thickness ratio (W/T) are listed in Table 1. The L/W ratio (aspect ratio) represents the degree of the lengthwise growth in the *c*-axis direction, while the W/T represents the shape of the cross section. OCP crystals grown without protein (control) were ribbon-like and the crystal had a length of 89.3±8.6μm, a width of 2011±596nm, and a thickness of 156±77nm[47]. In 10% rP148, crystal growth was restrained to form ribbon-like crystals that were smaller than control crystals. Their mean sizes were as follows: length 43±2μm; width 442±158nm; thickness 93±27nm (Table 1). The regulation of crystal growth by 10% rP148 was similar to previous observations of crystal growth regulation by 10% w/v of native bovine amelogenin, rM166, and rM179[48]. In contrast, in 40En solution, the length decreased remarkably (28±2μm) ($P<0.0001$), while the width (477±172nm) and the thickness (111±32nm) were almost the same as those obtained in 10% rP148 ($P = 0.19$ for width; $P = 0.03$ for thickness) (Table 1).

The regulatory effect of 32kDa enamelin on OCP crystal growth was modified in the presence of 10% rP148. In the mixture, the length decreased slightly, while the width decreased from 410±130nm (4En) to 148±51nm (10En) ($P<0.0001$), and then to 122±36nm (40En) ($P<0.002$) as the amount of enamelin added to the rP148 increased. As a result, L/W was 260±90 and W/T was 3.3±1.5 in the 10% rP148+10En; L/W was 286±91 and W/T was 1.7±0.7 in the 10% rP148+40En.

Figure 3 is a comparison of the L/W and W/T ratios of crystals grown in amelogenin gel-like matrix with and without enamelin addition. The L/W ratios of crystals grown both in rP148+10En and rP148+40En were significantly ($P<0.0001$) larger than those of other crystals. In contrast, the L/W ratio of crystals grown in En (58±21) was almost half that of crystals grown in rP148 (97±35) and almost a quarter of the L/W ratio of crystals grown in rP148+10En (260±90 and rP148+40En (286±91). The degrees of inhibitory action of rP148+4En (88±32nm) and rP148+40En (71±19nm) on thickness were almost the same ($P=0.15$). The thickness of crystals grown in rP148+10En (46±13nm) was the smallest seen under any of the conditions ($P<0.0001$). In contrast to the L/W ratio, the W/T ratios of crystals grown in rP148 (4.7±2.2) and 40En (4.3±2) were almost the same. In rP148/En mixed samples, the W/T ratio tended to decrease as enamelin concentration increased, resulting in the formation of prism-like crystals. Thus, OCP crystals grown in the 10% rP148+40En exhibited the largest L/W ratio ($P<0.0001$) and the smallest W/T ratio ($P<0.024$).

Our data demonstrate that the cooperative action of amelogenin rP148 and the 32kDa enamelin was critical for the growth of OCP crystals with a relatively large L/W ratio. Note that the aspect ratios of OCP crystals grown on the membrane without proteins are smaller

than those grew with amelogenin/enamelin mixture (see Table 1). The cooperative effect was dose dependent. These values are still smaller than aspect ratio of mature enamel crystals that are extremely long in their *c*-axial direction with an aspect ratio of approximately 1000[7]. Our observations suggest that other factors beside amelogenin and enamelin may contribute to the formation of unusually long crystals. In pure 32kDa enamelin solution (40En), OCP growth in the *c*-axis direction was greatly suppressed, and the L/W ratio of crystal was the smallest. Notably, when the same amount of the 32kDa enamelin was added to 10% rP148, the L/W ratio increased remarkably. We have previously proposed that amelogenin preferentially interacted with the (010) face of OCP, when compared with the (001) face47,48. As a result, the crystals became much narrower than crystals grown in the absence of amelogenin. In this study, although the concentration of enamelin added to amelogenin was very low, its effect on width was profound. Based on our recent finding that the 32kDa enamelin co-assembles with amelogenin stabilizing intermediate oligomers, we suggest that amelogenin-enamelin interaction enhanced the affinity of the complex to the (010) face31. As a result of the increased affinity of the amelogenin-enamelin complex for the (010) face, the crystals became much narrower than crystals that were formed in 10% rP148 without enamelin and/or in pure enamelin solution without rP148. Accordingly the L/W ratio became larger. This can be noted as a synergistic action of both proteins. Co-assembly of amelogenin and enamelin may result in conformational changes of the proteins leading to higher affinity for mineral surfaces66. Work is in progress to further investigate amelogenin-enamelin interactions and changes in configuration of these proteins as the results of their co-assembly (Fan et al, in preparation).

Small pseudo-spherical particles were apparent on crystal faces. Such particles were either aggregated (Fig 4a) or dispersed (Fig. 4b, 2b, 2c) and were not observed on crystals grown in 10% rP148, or 10%rP148+4En, nor in 40En solution. Since these particles were on the surface of the crystals, it can be expected that they contributed to the XRD spectra. Therefore, the possibility that these particles contributed to the XRD profile was examined by comparing the XRD profiles (Fig.1) of the products obtained in the presence of enamelin (rP148+4En, rP148+10En, rP148+40En and 40En) with that of the product obtained in rP148. Between 20° and 40° (2θ), the background intensity of the (rP148+10En and rP148+40En) was higher than those of the products obtained in rP148+4En and 40En (Fig S1, Supplementary material). Since ACP has broad XRD diffraction in the range of 20-40° with the maximum at around 30° (2θ)(CuK_{α})[38], it is possible that it may have caused the extra background intensity. Presumably, the source of the ACP in the products was the particles observed on the surface of the OCP crystals. Comparative analysis of X-ray diffraction patterns revealed larger quantities of ACP in the rP148+40En sample (Supplementary material, Fig S1) indicating that addition of enamelin to amelogenin enhances the potential of amelogenin to stabilize the ACP transient phase. Moreover, the size of these particles resembles ACP formed in *in vitro*[15,17,37,40-42] as well as those observed *in vivo*[34,36].

Considering recent findings that amelogenin stabilizes the ACP mineral phase *in vitro*[19] and that enamelin directly interacts with amelogenin *in vitro*[31], we cannot rule out that such particles may contain small amounts of proteins. The diameter of the particles was in the range between 100nm and 300nm, regardless of the protein concentrations. Large particles with a diameter of about 300-500nm were also observed on crystals (Fig.2d2). This suggested that the ratio of rP148 and the 32kDa En was crucial to stabilize the ACP containing particles.

EDXA mapping was performed on the small pseudo-spherical particles in the rP148+40En sample in order to elucidate whether they were calcium phosphate particles (Fig 5a-c). Both the calcium map (Fig 5b) and the phosphorus map (Fig 5c) clearly demonstrated that the

particles contained calcium and phosphorus. However, due to the close proximity of Au-M_α and P-K_α radiation (Observed at 2.120 keV and 2.013 keV respectively), the contrast between particles and background in the phosphorus map was diminished. Fig 5d shows an EDXA spectrum of the particles, highlighting the proximity of the Au and P signals. The particles show no crystalline structure and contain calcium and phosphorus. From these observations and the presence of a broad reflection in the XRD spectrum of the rP148+40En sample, the particles were deduced to be mainly amorphous calcium phosphate.

Conclusion

Using a double membrane system consisting of a cation selective membrane and dialysis membrane, we demonstrated that the rP148 amelogenin and the 32kDa enamelin cooperate to control the growth morphology of OCP crystals. Our findings have important implications for understanding the mechanism of lengthwise growth of enamel apatite crystals, which are eventually transformed to incipient ribbon-like crystallites during the maturation stage. General inhibition of the growth in the *b*-axis direction by enamelin and rP148 was comparable while enamelin inhibited the growth in the *c*-axis direction more effectively than rP148. When amelogenin and enamelin were mixed, the regulatory action of enamelin in the *c*-axis direction was diminished while that in the *b*-axis direction was emphasized resulting in the formation of longer and thinner crystals. In addition, the quantity of amorphous calcium phosphate phase detected after crystallization appeared larger when both rP148 and enamelin were used together. The concentration of enamelin was crucial for both the growth of OCP crystals with a large L/W ratio and for the stability of ACP phase. The cooperative regulation effect was attained presumably through direct binding of enamelin to rP148[24]. Cooperative interactions between amelogenin and enamelin fragments could be critical for controlling the morphology of enamel crystals in the post-secretory stage. Understanding the details of such control mechanisms will prepare the ground for the development of improved biomaterials.

Supplementary Material

Refer to Web version on PubMed Central for supplementary material.

Acknowledgments

This study was supported by NIH-NIDCR R01 grants DE-13414, DE-15644 to JMO.

References

1. Lowenstam, HA.; Weiner, S. On Biomineralization. Oxford University Press; New York: 1989.
2. Moradian-Oldak, J.; Paine, ML. Metal Ions In Life Sciences. Astrid, Sigel; Sigel, H.; Sigel, RKO., editors. Vol. 4. John Wiley & Sons, Ltd; Chichester: 2008. p. 507-546.Biomineralization. From Nature to Application
3. Veis A. Science. 2005; 307:1419–1420. [PubMed: 15746414]
4. Fearnhead RW. Nature. 1960; 189:509. [PubMed: 13698485]
5. Ronnholm E. J. Ultrastruct. Res. 1962; 6:249–303. [PubMed: 14493689]
6. Nylen MU, Eanes ED, Omnel KA. J. Cell Biol. 1963; 18:109–123. [PubMed: 13939321]
7. Daculsi G, Menanteau G, Kerebel LM, Mitre D. Calcif Tissue Int. 1984; 36:550–555. [PubMed: 6441627]
8. Eastoe, JE. Advan. Fluorine Res. Dent. Caries Preven. Vol. 3. Pergamon Press; Oxford: 1965. p. 5-17.
9. Fincham AG, Moradian-Oldak J, Simmer JP, Sarte PE, Lau EC, Diekwisch T, Slavkin HC. J. Struct. Biol. 1994; 112:103–109. [PubMed: 8060728]

10. Moradian-Oldak J, Simmer JP, Lau EC, Sarte PE, Slavkin HC, Fincham AG. Biopolymers. 1994; 34:1339–1347. [PubMed: 7948720]
11. Margolis HC, Beniash E, Fowler CE. J. Dent. Res. 2006; 85:775. [PubMed: 16931858]
12. Moradian-Oldak J, Du C, Falini G. Eur. J. Oral Sci. 2006; 114:289–296. [PubMed: 16674701]
13. Robinson C, Fuchs P, Weatherell JA. J Crystal Growth. 1981; 53:160–165.
14. Fincham AG, Moradian-Oldak J, Diekwisch T, Simmer JP, Sarte PE, Lyaruu DM, Slavkin HC. J. Struct. Biol. 1995; 115:50–59. [PubMed: 7577231]
15. Wang L, Guan X, Du C, Moradian-Oldak J, Nancollas GH. J. Phys. Chem. 2007; 111:6398–6404.
16. Tarasevich BJ, Howard CJ, Larson JL, Snead ML, Simmer JP, Paine M, Shaw WJ. J. Struct. Biol. 2007; 304:407–415.
17. Yang X, Wang L, Qin Y, Sun Z, Henneman ZJ, Moradian-Oldak J, Nancollas GH. J. Phys. Chem. B. 2010; 114(6):2293–22300. [PubMed: 20104924]
18. Beniash E, Simmer JP, Margolis HC. J. Struct. Biol. 2005; 149:182–190. [PubMed: 15681234]
19. Kwak SY, Wiedemann-Bidlack FB, Beniash E, Yamakoshi Y, Simmer JP, Litman A, Margolis HC. J. Biol. Chem. 2009; 284(28):18972–18979. [PubMed: 19443653]
20. Termine JD, Belcourt AB, Christener PJ, Conn KM, Nylen MU. J. Biol.Chem. 1980; 255:9760–9768. [PubMed: 7430099]
21. Yanagisawa T, Nylen MU, Termine JD. J. Dent. Res. 1981; 60A:558.
22. Tanabe T, Aoba T, Moreno C, Fukae M, Shimizu M. Calcif. Tissue Int. 1990; 46:205–215. [PubMed: 2106381]
23. Hu CC, Hu Y, Smith CE, McKee MD, Wright JT, Yamakoshi Y, Papagerakis P, Hunter GK, Feng JQ, Yamakoshi F, Simmer JP. J. Biol. Chem. 2009; 283:10858–10871. [PubMed: 18252720]
24. Hu CC, Yamakoshi Y. Crit. Rev. Oral Biol. Med. 2003; 14:387–398. [PubMed: 14656895]
25. Fukae M, Tanabe T, Murakami C, Dohi N, Uchida T, Shimizu M. Adv Dent Res. 1996; 10:111–8. [PubMed: 9206327]
26. Dohi N, Murakami C, Tanabe T, Yamakoshi Y, Fukae M, Yamamoto Y, Wakida K, Shimizu M, Simmer JP, Kurihara H, Uchida T. Cell Tissue Res. 1998; 293:313–25. [PubMed: 9662654]
27. Yamakoshi Y. Calcif. Tissue Int. 1995; 56:323–330. [PubMed: 7767845]
28. Rajpar MH, Harley K, Laing C, Davies RM, Dixon MJ. Hum. Mol. Genet. 2001; 10:1673–1677. [PubMed: 11487571]
29. Kida M, Ariga T, Shirakawa T, Oguchi H, Sakiyama Y. J Dent Res. 2002; 81:738–42. [PubMed: 12407086]
30. Bouropooulos N, Moradian-Oldak J. J Dent. Res. 2004; 83:278–282. [PubMed: 15044499]
31. Fan D, Du C, Sun Z, Lakshminarayanan R, Moradian-Oldak J. J. Struct. Biol. 2009; 166(1):88–94. [PubMed: 19263522]
32. Weiner S, Sagi I, Addadi L. Science. 2005; 309:1027–1028. [PubMed: 16099970]
33. Crane NJ, Popescu V, Morris MD, Steenhuiss P, Ignelzi MA. Bone. 2006; 39:434–442. [PubMed: 16627026]
34. Mahamid J, Sharir A, Addadi L, Weiner S. Proc. Nat. Acad. Sci. 2008; 105(35):12748–12753. [PubMed: 18753619]
35. Gower LB. Chem. Rev. 2008; 108:4551–4627. [PubMed: 19006398]
36. Beniash E, Metzler RA, Lam RSK, Gilbert PUPA. J.Struct.Biol. 2009; 166:133–143. [PubMed: 19217943]
37. Tao J, Pan H, Zeng Y, Xu X, Tang R. J. Phys. Chem.B. 2007; 111:13410–13418. [PubMed: 17979266]
38. Eanes ED, Gillessen IH, Posner AS. Nature. 1965; 28:365–367. [PubMed: 5885449]
39. Termine JD, Peckauskas RA, Posner AS. Arch. Biochem. Biophys. 1970; 140:318–325. [PubMed: 4319593]
40. Boskey AL, Posner AS. J.Phys.Chem. 1973; 77:2312–2317.
41. Nylen MU, Eanes ED, Termine JD. Calcif. Tiss. Res. 1972; 9:95–108.
42. Eanes ED, Termine JD, Nylen MU. Calcif. Tiss. Res. 1973; 12:143–148.

43. Meyer JL, Eanes ED. Calcif. Tiss. Res. 1978; 25:59–68.
44. Brown WE, Smith JP, Lehr JR, Frazier AW. Nature. 1962; 196:1048–1055.
45. Brown, WE. Tooth Enamel II. Stack, MV.; Fearnhead, RW., editors. John Wright Ltd.; Bristol: 1965. p. 11-14.
46. Chickerur NW, Tung MS, Brown WE. Calcif Tiss Int. 1980; 32:55–62.
47. Iijima M, Hayashi K, Moriwaki Y. J. Crystal Growth. 2002; 234:539–544.
48. Iijima M, Moriwaki Y, Takagi T, Moradian-Oldak J. J. Crystal Growth. 2001; 222:615–626.
49. Iijima M, Moriwaki Y, Wen HB, Fincham AG, Moradian-Oldak J. J. Dent. Res. 2002; 81:69–73. [PubMed: 11820371]
50. Iijima M, Moradian-Oldak J. Calcif. Tiss. Int. 2004; 74:522–531.
51. Iijima M, Moradian-Oldak J. J.Mater.Chem. 2004; 14:2189–2199.
52. Iijima M, Moradian-Oldak J. Biomaterial. 2005; 26:1595–1603.
53. Moradian-Oldak J. Matrix Biol. 2001; 20:293–305. [PubMed: 11566263]
54. Sun Z, Ahsan MM, Wang H, Du C, Abbott C, Moradian-Oldak J. Eur. J. Oral Sci. 2006; 114(Suppl. 1):59–63. (discussion 93–95, 379–380). [PubMed: 16674664]
55. Ryu, O.; Yamakoshi, Y.; Cao, X.; Zhang, C.; Villemain, JL.; Simmer, J.; Hu, CC. The 8th international symposium on biomineralization (BIOM2001). I.; K.; H.; O., editors. Tokai University Press; Niigata, Japan: 2001.
56. Yamakoshi Y, Phinheiro FHS, Tanabe T, Fukae M, Shimizu M. Connect. Tiss. Res. 1998; 39:39–46.
57. Uchida T, Tanabe T, Fukae M, Shimizu M. Arch. Histol. Cytol. 1991; 54:527–538. [PubMed: 1793666]
58. Robinson C, Fuchs P, Deutsch D, Weatherell JA. Caries Res. 1978; 12:1–11. [PubMed: 271519]
59. Aoba T, Moreno EC. Calcif Tissue Int. 1987; 41:86–94. [PubMed: 3115550]
60. Tan J, Leung W, Moradian-Oldak J, Zeichner-David M, Fincham AG. J Dent Res. 1998; 77:1388–96. [PubMed: 9649167]
61. Ryu OH, Fincham AG, Hu CC, Zhang C, Qian Q, Bartlett JD, Simmer JP. J. Dent. Res. 1999; 78:743–750. [PubMed: 10096449]
62. Fan D, Lakshminarayanan R, Moradian-Oldak J. J Struct Biol. 2008; 163:109–15. [PubMed: 18508280]
63. Fearnhead, R.; Kawasaki, K. Mechanisms and Phylogeny of Mineralization in Biological Systems. Springer; New York: 1991. p. 79-81.
64. Hata M, Moriwaki Y, Doi Y, Goto T, Wakamastu N, Kamemizu H. J. Jpn Assocoation for Crystal Growth. 1985; 12:91–99.
65. Elliott, JC,G. PAYS-BAS. Vol. 18. Elsevier; Amsterdam: 1994. p. XIIIp. 389
66. Hunter GK, O'Young J, Grohe B, Karttunen M, Goldberg HA. Langmuir. Jun 8.2010 [Epub ahead of print].

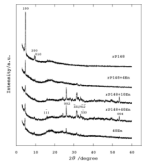

Figure 1.
X-ray diffraction patterns of the products grown in (a) 10% rP148, (b) 4μg/ml enamelin in 10% rP148 (rP148+4En), (c) 10μg/ml enamelin in 10% rP148 (rP148+10En), (d) 40μg/ml enamelin in 10% rP148 (rP148+40En) and (e) 40μg/ml enamelin (40En).

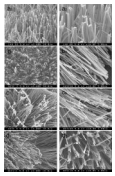

Figure 2.
SEM images of small particles adhere to crystals grown in (a)10μg/ml enamelin in 10% rP148 (rP148+10En) and (b) 40μg/ml enamelin in 10% rP148 (rP148+40En).

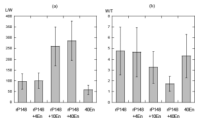

Figure. 3.

(a) Length to width (L/W) ratio and (b) width to thickness (W/T) ratio of crystals grown in 10% rP148, 4μg/ml enamelin in 10% rP148 (rP148+4En), 10μg/ml enamelin in 10% rP148 (rP148+10En), 40μg/ml enamelin in 10% rP148 (rP148+40En) and 40μg/ml enamelin (40En).

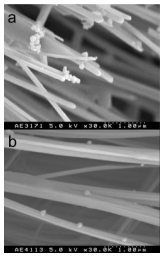

Figure 4.
SEM images of the products grown in amelogenin with increasing concentration of the 32kDa enamelin (a) 10% rP148, (b) 40μg/ml enamelin (40En), (c) 10μg/ml enamelin in 10% rP148 (rP148+10En) and (d) 40μg/ml enamelin in 10% rP148 (rP148+40En). In (d2), it is important to note that the small particles adhered to crystals. (a1-d1 are at a magnification of 3K and a2-d2 are at a magnification of 10K).

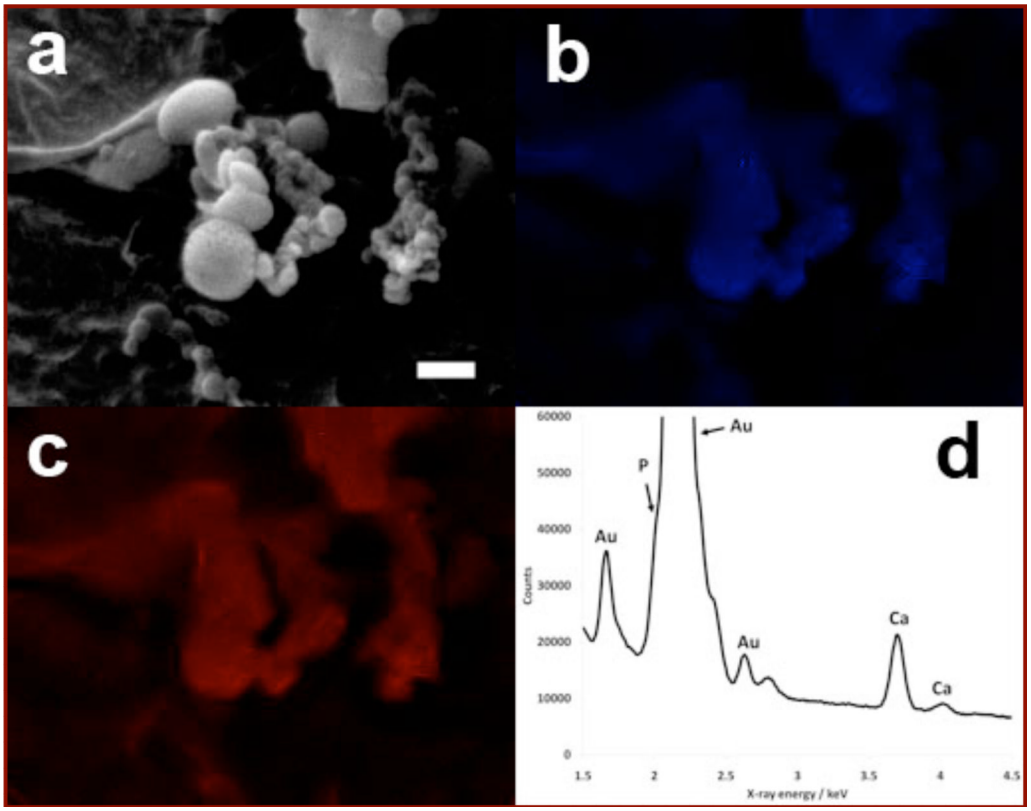

Figure 5.

SEM images and EDXA mapping of the pseudo-spherical particles observed in the rP148+40En sample. The brightness and contrast of the EDXA maps were altered for clarity. (a) A low resolution SEM image of the area that was mapped. Scale bar 500nm. (b) The EDXA map of calcium (Ca-K_α x-ray radiation at 3.691 keV). (c) The EDXA map of phosphorus (P-K_α x-ray radiation at 2.013 keV). It is important to note that the sample was coated in gold and some of the phosphorus signal may have come from Au-M_α x-ray radiation at 2.120 keV, although the Au-M_α and P-K_α spectral windows do not overlap. (d) The EDXA spectrum of the particles. The calcium K_α and K_β peaks are clearly visible, but the phosphorus K_α peak only appears as a shoulder on the side of a large gold M_α peak.

Table 1

Mean values of length (L), width (W), thickness (T), L/W and W/T ratio of crystals grown in 10% rP148, 4μg/ml enamelin in 10% rP148 (rP148+4En), 10μg/ml enamelin in 10% rP148 (rP148+10En), 40μg/ml enamelin in 10% rP148 (rP148+40En) and 40μg/ml enamelin (40En). These values were compared by paired-sample t-test (Welch's method) at α=0.05. A paired-sample (indicated by alphabet; a, b) was picked from different concentrations within each column. When P value was <0.05, they were considered to be significantly different. Some pairs of data that gave 0.001< P < 0.1 are presented in the footnote. For example, the W/T ratio of rP148 and rP148+10En (both are labeled with W/Ta) was judged statistically not different with the P value of 0.002. The crystal size and the aspect ratios of OCP crystals grown in the absence of the proteins are given in the last line as no addition[47].

Proteins	Length μm	Width nm	Thickness nm	L/W	W/T
rP148	43±2	442± 158	93±27 Ta, b	97±35	4.7±2.2 W/Ta
rP148+4En	41±7	410± 131	88± 32	100± 36	4.6±2.3 W/Tb
rP148+10En	39± 2La	148± 51	46± 13	260±90L/Wa	3.3±1.5 W/Ta,b
rP148+40En	35± 4La	122± 36	71± 29 Tb	286±91 L/Wa	1.7± 0.7
40En	28± 2	477±172	111± 32 Ta	58±21	4.3±2.0
no addition	89± 8	2011± 596	156± 78	44±14	13± 7

P_{La}=0.002, necessary to show these values are statistically different.

P_{Ta}=0.03, PTb=0.005, necessary to show these values are statistically different.

$P_{L/Wa}$=0.1005, these are statistically different, but P value is not large.

$P_{W/Ta}$=0.059, PW/Tb=0.061, these are statistically different, but P value is not large.

Cryst Growth Des. Author manuscript; available in PMC 2011 November 1.